

Spin-Polarized Transient Electron Trapping in Si:P

Yuan Lu,^{*} Jing Li, and Ian Appelbaum[†]

*Department of Physics and Center for Nanophysics and Advanced Materials,
University of Maryland, College Park MD 20742 USA*

An unexpected source of nonequilibrium spin dephasing in n-type phosphorus-doped silicon is observed when temperature and voltage conditions provide a confining electrostatic potential conduction band profile between injector and detector Schottky barriers. In addition to Hanle spin precession features for magnetic fields in the kOe range, we also observe substantial (but incomplete) dephasing with much smaller characteristic widths of ≈ 50 -100 Oe. The possibility that this phenomenon originates from transit-time delays associated with capture/re-emission in shallow impurity traps is discussed in light of temperature, voltage, and electron density dependence measurements, and is supported by a numerical model.

Incorporating impurities into the otherwise pure silicon (Si) lattice has numerous consequences for charge transport. Most importantly, doping using atomic species with more than Si's four valence electrons not only provides mobile charge to the conduction band, but also leaves behind a positively-charged ion that modifies the electrostatic energy landscape when not screened. But beyond impacting the flow of electron charge, electron (or n-type) doping also impacts spin-polarized transport as well.[1–3]

For example, several years ago we showed how band bending gives rise to non-ohmic spin transport in ≈ 3 μm -thick n-type lightly phosphorus-doped Si using all-electrical ballistic hot electron injection and detection techniques.[4] In the present work, we show that the under certain circumstances, a mechanism of low-magnetic-field spin dephasing not seen in otherwise-equivalent undoped devices[5, 6] can be induced in lowly-doped channel regions of vertical-transport systems. These results are attributed to the interaction of conduction electrons with shallow impurity-related traps and suggest that the study of spin-polarized transport in semiconductors can potentially be used to elucidate fast processes previously accessible only to time-domain techniques.

The devices we use here are nominally identical to the those in Ref. 4, but with slightly lower impurity density. Previous measurements have indicated that the confluence of Schottky depletion regions on both injector and detector sides of the transport channel result in a confining conduction-band profile (i.e. an electrostatic potential energy minimum exists) for applied voltages (V_{C1}) below ≈ 2 V at temperatures sufficient to ionize the dopants.[7] Assuming full depletion, this corresponds to a doping density of approximately $3 \times 10^{14} \text{ cm}^{-3}$; a schematic band-diagram of this device scenario is shown in Fig. 1.

Fig. 2 shows spin transport signals from these devices in a nearly perpendicular magnetic field as a function of temperature for $V_{C1} = 1.5\text{V}$. Because of the intentional misalignment of several degrees from perpendicular orientation, a small in-plane field component switches the in-plane magnetizations of injector and detector fer-

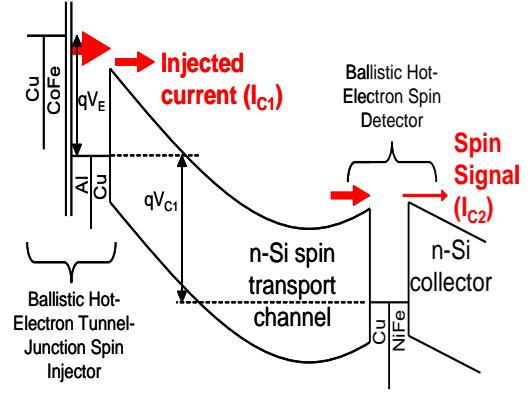


FIG. 1: Schematic band diagram of vertical n-type doped Si spin transport channel devices used in this work, showing band-bending and the resultant potential minimum for temperatures high enough to ionize dopants and low applied voltage V_{C1} .

romagnets, superimposing spin-valve features of signals under parallel and anti-parallel configurations on the spin precession lineshape.

At low temperature [35K, shown in Fig. 2 (a)], the phosphorus impurities are neutralized by “frozen” bound electrons and the low density of fixed space charge results in a flat conduction band profile. Transport across 3 μm Si thus requires an average transit time \bar{t} of only $\approx 50\text{ps}$. Such short transit times require large precession frequencies $\omega = g\mu_B B/\hbar$ to appreciably rotate spin orientation (where g is the electron spin g-factor, μ_B is the Bohr magneton, B is the magnetic field, and \hbar is the reduced Planck constant). Hence, the precession minima due to $\theta = \omega\bar{t} = \pi$ rad rotation (i.e. a full spin flip) are at a relatively large value of $B \gtrsim 3.5$ kOe, indicated by vertical black arrows.

As temperature increases to 45K in Fig. 2(b), a decrease in mobility and the onset of partial donor ionization and band-bending results in reduction of the precession minima field to ≈ 3 kOe. By comparison to results from the highest temperature [shown in Fig. 2 (f), at 85K], it appears as though this trend of coher-

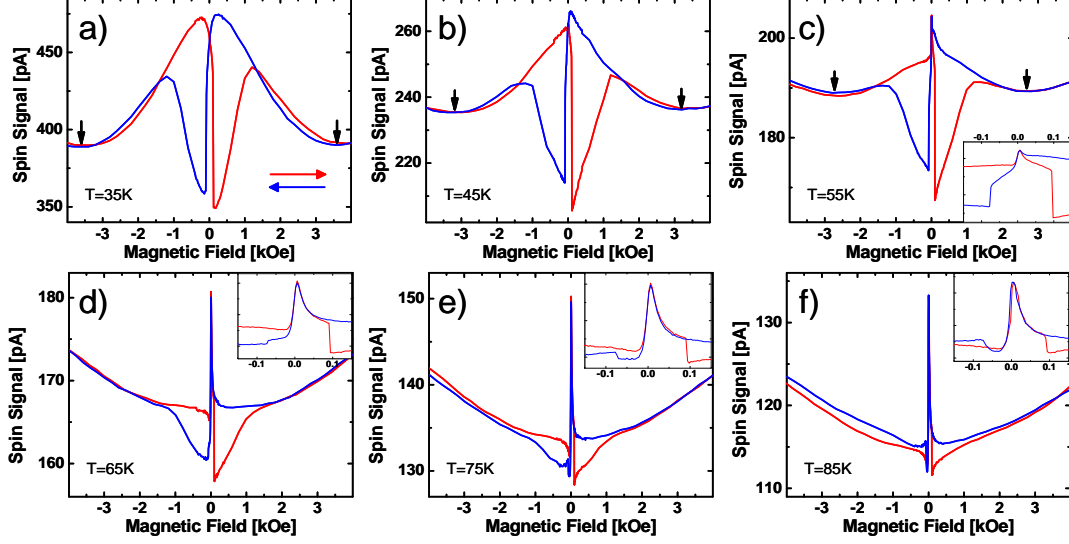


FIG. 2: Temperature dependence of spin transport signal in a nearly perpendicular magnetic field from 35K-85K [(a)-(f)] at an applied voltage between injector and detector $V_{C1}=1.5\text{V}$. Vertical arrows indicate fields where average spin precession angle is π rad. Insets for (c)-(f) show low-field magnification of the same data.

ent precession features falling to lower magnetic fields due to longer transit times and spin dephasing has resulted in a very narrow spin signal peak of width only ≈ 100 Oe. [The slow signal increase at large fields is the result of out-of-plane magnetization rotation when the perpendicular field strength compares with the thin-film shape anisotropy.]

However, at intermediate temperatures starting in the 55K regime, it is evident that our spin transport signal includes the signatures of two *distinct* processes: both (i) coherent precession giving rise to precession minima at several kOe, and (ii) a low-field dephasing resulting in a narrow, slightly asymmetric peak of width 50-100 Oe shown in the insets to Figs. 2 (c)-(f). Even at 65K and 75K, it is clear through the persistence of the spin-valve splitting to ≈ 1 kOe that the sharp peak centered at zero field does not entirely dephase the spins. Only at temperatures greater than 85K shown in Fig. 2(f) does the low-field peak account for nearly the entire signal magnitude. Therefore, we attribute this spin dephasing effect to a heretofore unseen mechanism.

To investigate the origin of this effect, we now focus on the low-field regime. To avoid the impact of spin-valve switching due to slight geometrical misalignment in the low-field region of our spin signal seen in Fig. 2, we orient the magnetic field as precisely perpendicular to the device as possible in our cryostat. The resulting reduction in in-plane field component pushes the switching features of the spinvalve effect to >500 Oe. In this configuration, the magnetization of the harder magnetic layer (in this case, CoFe in the spin injector tunnel junc-

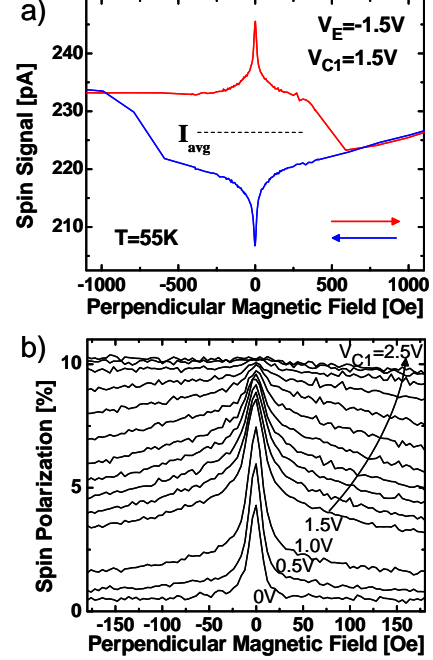


FIG. 3: Perpendicular-field measurements at 55K. In (a), a full field loop displays square hysteresis and clear low-field dephasing without the asymmetry and magnetization reversal shown in Fig. 2. In (b), voltage dependence of the low-field signal is shown, where the applied voltage V_{C1} is changed from 0V, 0.5V, 1.0V, and 1.5V to 2.5V in steps of 0.1V.

tion cathode) remains fixed, and our measurements (as shown at $T=55\text{K}$ in Fig. 3 (a)) show an open loop. The small-field peak in parallel magnetization configuration (left-to-right sweep, red) becomes inverted for the antiparallel configuration (right-to-left sweep, blue).

When the applied voltage between injector and detector (V_{C1}) is changed, the shape of the small-field peak also changes. In Fig. 3(b), we show the low-field region of our measurements from parallel magnetization (I_P), where changes in absolute signal current as a function of applied voltage are eliminated by plotting spin polarization $(I_P - I_{avg})/I_{avg}$, where I_{avg} is the average between parallel and anti-parallel signals, as shown by the horizontal dotted line in Fig. 3(a). Clearly, higher applied voltage corresponds to a widening peak that accounts for less of the total signal. At voltages sufficient to entirely remove the confining potential in the conduction band (e.g. $V_{C1}=2.5\text{V}$), the low-field peak disappears entirely.

This low-field feature is reminiscent of similar observations in optical[8] and transport[9] measurements of spin-polarized electrons in GaAs. In that case, the phenomena was attributed to a non-linear dynamic feedback between electron spin and nuclear spin via Overhauser and Knight fields.[10] Ref. 9, for instance, demonstrates a remarkable degree of correspondence with steady-state fine-difference time-domain calculations of spin transport in the presence of the self-consistent nuclear field, and its modification by microwave excitation resonant with the nuclear spin splitting. That effect also has a strong sensitivity to magnetic field misalignment, and the asymmetry of the peaks in the insets to Figs. 2 (c)-(f) is also suggestive of a common cause (although here it is partially obscured by magnetization switching from in-plane field components).

Despite the similarity, however, there are several reasons to disregard this mechanism as a possible origin. Si is expected to have much weaker hyperfine interactions than GaAs due to the small relative abundance of nonzero nuclear spin isotopes ($\approx 5\%$ for spin- $1/2$ ^{29}Si ; spin- $1/2$ ^{31}P dopants are even more dilute). In comparison, every nucleus in GaAs has nonzero spin. Furthermore, the model predicts that the sign of the misalignment-induced asymmetry inverts when the injected spin orientation switches; this is contrary to observations in the insets to Figs. 2 (c)-(f).

Our spin current signal is essentially a measurement of the average spin precession angle θ , which is a product of both spin precession frequency ω and transit time t . In principle, the effects discussed above could be the result of modification of either of these; a linear process would require that there is a sub-ensemble of electrons either moving substantially slower or precessing substantially faster than the rest to account for both large- and small-field features.

Because the existence of g-factors significantly greater than 2 are unheard-of in Si, we suggest that the origin

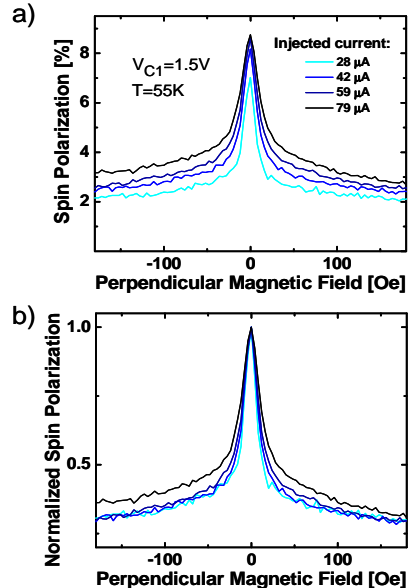


FIG. 4: Low-field dephasing as a function of injected current and hence steady-state electron density. In (a), spin polarization is shown, whereas (b) demonstrates a reduction in relative contribution to the overall signal from trapped electrons when density increases.

of our observations is a transit-time effect due to the presence of trapping and subsequent re-emission of spin-polarized conduction electrons in shallow impurity states. At typical injection currents of $\approx 10\text{ }\mu\text{A}$, there are approximately 10^{14} electrons entering (and leaving) this volume each second. For a quasi-Lorentzian Hanle half-width at half-maximum of $\Delta B \approx 50\text{ Oe}$, an average transit time of $\hbar/(g\mu_B\Delta B) = 1\text{ ns}$ implies a steady-state population of 10^5 occupied traps in the channel. This value is below the actual density of approximately 10^7 available charged impurities under conditions above the ionization temperature in the effective volume $\approx 100\text{ }\mu\text{m} \times 100\text{ }\mu\text{m} \times 3\text{ }\mu\text{m}$ at the phosphorus density used here (although this number must be reduced at low temperatures due to nonzero occupation probability).

By varying the electron density via injected current (I_{C1}), we can see the signature of this fixed trap number. Although the available range of this parameter is limited by the reliable operating conditions of our tunnel junction spin injector, one can clearly see in Fig. 4(a) that the overall polarization increases with injected current. When these polarization measurements are normalized to the $B=0$ value in Fig. 4(b), it becomes apparent that a small but substantial decrease in the relative proportion of trapped electrons (i.e. relative peak height to background polarization) accompanies an increase in conduction electrons as well. This behavior indicates a possible approach to saturation of the impurities and a

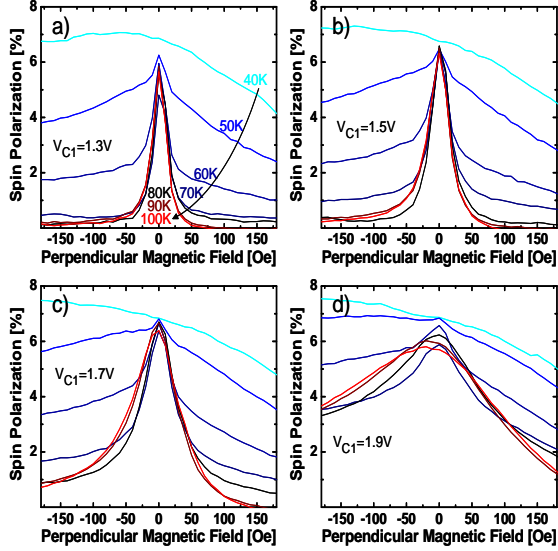


FIG. 5: Temperature dependence of low-field dephasing between 40K and 100K at applied voltages $V_{C1} = 1.3\text{V}$ (a), 1.5V (b), 1.7V (c), and 1.9V (d).

fixed contribution to low-field dephasing.

Temperature dependence of this phenomenon is shown in Figs. 5(a)-(d). Here, we see that although temperature does indeed modify the relative contribution to the overall signal, the linewidth is only slightly modified over a wide range of applied voltages. The increase in width accompanying increases in applied voltage V_{C1} – especially at elevated temperature – are presumably the result of partial field ionization which decreases dwell time in the trap.

Average transit times for electrons participating in trapping events of approximately 1ns (indicated by the width of the low-field peak) are relatively small for the expected ground-state phosphorus-impurity trap depth of 45meV.[11] Consistency of the present trapping model with the observed timescales requires the participation of trapping-emission cycles involving long-lived, shallow states that are presumably excited Rydberg states distinct from the relatively deep ground state. In this regard, it is supportive to note that recent time-domain experiments with a far-infrared pulsed free-electron laser has identified lifetimes of the phosphorus $2p_0$ excited state (11.5meV below the conduction band) exceeding 200ps in this temperature range.[12] Recent calculations suggest an intrinsic timescale of over 1ns,[13] which has even enabled population inversion and lasing in externally-pumped systems.[14]

A simple numerical model designed to capture the observed behavior considers the convolution of all $0 \leq k \leq N$ possible trapping events in N available traps with trapping probability α .

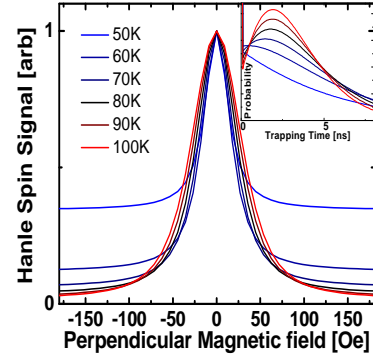


FIG. 6: Simulated spin-precession Hanle signals using the trapping-time model (Eq. 1) with parameters $\alpha=0.1$, $\tau_0=200\text{ps}$, $\Delta E=11.5\text{meV}$, and effective 1-d current of 3nA sampling $N=100$ traps. Compare with corresponding experimental results in Fig. 5. Inset: Calculated trapping-time distributions.

$$(1 - \alpha P_E)^N \delta(t) + \sum_{k=1}^N \binom{N}{k} (1 - \alpha P_E)^{N-k} (\alpha P_E)^k G(t, k, \tau_t) \quad (1)$$

where $G(t, k, \tau_t)$ is the gamma probability distribution (convolution of k exponentials of trapping timescale τ_t).

The probability of an empty trap (P_E) is given by the relative ratio of incident timescale (τ_i determined by the effective 1-d current), to trapping timescale ($\tau_t = \tau_0 e^{\Delta E/k_B T}$) such that $P_E = 1 - \frac{\tau_t}{\tau_i + \tau_t}$. Correspondence of this model's numerical predictions to the general features of experimental data are shown in Fig. 6, where the changes in trapping contribution and weak linewidth dependence on temperature observed in experimental results (Fig. 5) are clearly captured.

Although we attribute the observed low field behavior to transient trapping effects, more research on this phenomena is required to elucidate the detailed mechanism and reconcile discrepancies with the expectations of a simple quantitative theory. In particular, a trapping mechanism by itself is not expected to explain the observed sensitivity to field geometry; small magnetic field deviation from perfect perpendicular alignment of only several degrees in Fig. 2 give rise to large signal asymmetries, whereas these should be absent to first order.[15]

The explicit coupling of spin-polarized conduction electrons with phosphorus impurities as demonstrated here opens many research possibilities. Once a successful and truly quantitative theory is developed, it may be useful as a spectroscopic probe of impurity levels and transition rates not explicitly requiring time-domain methods as previously assumed were necessary.[12] In addition, we speculate that it may become possible to explore the role of contact hyperfine interactions and dynamic nuclear polarization of the phosphorus nuclear spin by itinerant non-equilibrium spin-polarized conduction electrons with

NMR techniques for potential application to quantum computing schemes.[16]

We acknowledge helpful comments by S. Bohacek. This work was supported by the Office of Naval Research and the National Science Foundation. We acknowledge the support of the Maryland NanoCenter and its FabLab.

* Present address: CNRS Institut Jean Lamour, Nancy, FR

† appelbaum@physics.umd.edu

- [1] R. Jansen, B. C. Min, S. P. Dash, S. Sharma, G. Kioseoglou, A. T. Hanbicki, O. M. J. van 't Erve, P. E. Thompson, and B. T. Jonker, *Phys. Rev. B* **82**, 241305 (2010).
- [2] O. van 't Erve, A. Hanbicki, M. Holub, C. Li, C. Awo-Affouda, P. Thompson, and B. Jonker, *Appl. Phys. Lett.* **91**, 212109 (2007).
- [3] T. Sasaki, T. Oikawa, T. Suzuki, M. Shiraishi, Y. Suzuki, and K. Noguchi, *Appl. Phys. Lett.* **96**, 122101 (2010).
- [4] H.-J. Jang, J. Xu, J. Li, B. Huang, and I. Appelbaum, *Phys. Rev. B* **78**, 165329 (2008).
- [5] I. Appelbaum, B. Huang, and D. J. Monsma, *Nature* **447**, 295 (2007).
- [6] B. Huang, D. J. Monsma, and I. Appelbaum, *Phys. Rev. Lett.* **99**, 177209 (2007).
- [7] Y. Lu and I. Appelbaum, *Appl. Phys. Lett.* **97**, 162501 (2010).
- [8] D. Paget, G. Lampel, B. Sapoval, and V. I. Safarov, *Phys. Rev. B* **15**, 5780 (1977).
- [9] M. K. Chan, Q. O. Hu, J. Zhang, T. Kondo, C. J. Palmström, and P. A. Crowell, *Phys. Rev. B* **80**, 161206 (2009).
- [10] A. W. Overhauser, *Phys. Rev.* **92**, 411 (1953).
- [11] S. Sze, *Physics of Semiconductor Devices, 2nd edition* (Wiley-Interscience, New York, 1981).
- [12] N. Vinh, P. Greenland, K. Litvinenko, B. Redlich, A. van der Meer, S. Lynch, M. Warner, A. Stoneham, G. Aeppli, D. Paul, et al., *Proc. Natl. Acad. Sci. USA* **105**, 10649 (2008).
- [13] V. Tyuterev, J. Sjakste, and N. Vast, *Phys. Rev. B* **81**, 245212 (2010).
- [14] S. G. Pavlov, R. K. Zhukavin, E. E. Orlova, V. N. Shastin, A. V. Kirsanov, H.-W. Hübers, K. Auen, and H. Riemann, *Phys. Rev. Lett.* **84**, 5220 (2000).
- [15] J. Li, B. Huang, and I. Appelbaum, *Appl. Phys. Lett.* **92**, 142507 (2008).
- [16] H. Morishita, L. S. Vlasenko, H. Tanaka, K. Semba, K. Sawano, Y. Shiraki, M. Eto, and K. M. Itoh, *Phys. Rev. B* **80**, 205206 (2009).